

1 **Surface area is the biologically most effective dose metric for acute**
2 **nanoparticle toxicity in the lung**

3

4 Otmar Schmid, Tobias Stoeger

5

6 Comprehensive Pneumology Center, Member of the German Center for Lung Research, Max-Lebsche-
7 Platz 31, 81377 Munich, Germany

8 Institute of Lung Biology and Disease, Helmholtz Zentrum München, 85764 Neuherberg, Germany

9

10 **Corresponding author:**

11 Otmar Schmid

12 Phone: ++49-89-3187-2557

13 Email: otmar.schmid@helmholtz-muenchen.de

14

15

16 **Key words (ideas):**

17 Nanotoxicology, inflammation, lung, dose-response, in vivo, surface area, dose metric, inhalation exposure,
18 risk assessment

19

20 **Abstract**

21 In this study we provide guidance on the biologically most relevant dose metric for pulmonary toxicity of
22 biopersistent, spherical nanoparticles (NPs). A retrospective analysis of nine *in vivo* studies on particle-
23 induced, acute pulmonary toxicity in animal models (mouse, rat) was performed encompassing five
24 different types of nanomaterials (polystyrene, titanium dioxide, carbonaceous materials, transition
25 metal oxides (Co, Ni, Zn) and hydrothermally synthesized α -quartz) with a wide range of primary particle
26 diameters (9-535 nm) and mass-specific BET surface areas (6-800 m²/g). The acute influx of
27 polymorphonuclear cells (PMNs) into the lungs after intratracheal instillation of NPs was chosen as
28 toxicological endpoint for acute lung inflammation. The allometrically scaled toxicological data were
29 investigated with respect to various dose metrics, namely (primary) particle number, joint length, BET
30 and geometric surface area, volume and mass.

31 Surface area is identified as the biologically most relevant dose metric for spherical NPs explaining about
32 80% of the observed variability in acute pulmonary toxicity ($R^2 = 0.77$). None of the other dose metrics
33 explains more than 50% of the observed variability in pulmonary inflammation. Moreover, using surface
34 area as the dose metric allows identification of materials with different specific toxicity independent of
35 particle size. Typical materials without intrinsic toxicity - here referred to as low-solubility, low-toxicity
36 (LSLT) materials - show low surface-specific toxicity with an EC₅₀ dose of 175 m²/g-lung (geometric
37 mean; $\sigma_g = 2.2$), where EC₅₀ represents the dose inducing 50% of the maximum effect (here: 30% PMN).
38 In contrast, transition metal oxides (here: Co, Ni, Zn) - materials known for their intrinsic toxicity -
39 display 12-fold enhanced surface-specific toxicity compared to LSLT particles (EC₅₀ = 15 m²/g-lung).

40 This analysis implies that surface-related modes of action are driving acute pulmonary toxicity for the
41 types of NPs investigated here. The relevance of other dose metrics such as number and volume is
42 acknowledged in the context of different modes of action, namely shape-induced toxicity (fiber

43 paradigm) and extremely high particle lung burden (overload conditions), respectively. So which dose
44 metric should be monitored by aerosol scientists involved in health related aerosol exposure
45 measurements? The short answer is – all of them (except length), but there is a strong preference
46 towards surface area.

47

48 **1. Introduction**

49 Epidemiological studies have described correlations between the mass concentration of ambient
50 particulate matter (PM) and increased morbidity and mortality in adults and children (Salvi, 2007; V.
51 Stone, Johnston, & Clift, 2007). The tremendous economic success of consumer products containing
52 nanomaterials (e.g. sun screen, tooth paste, tires) has raised concerns regarding consumer exposure to
53 inhaled nanostructured materials. However, very little epidemiological data are available for engineered
54 nanomaterials. The few studies performed at industrial sites of nanoparticle (NP) production (mainly
55 carbon black) did not show conclusive evidence of particle-induced health effects (Boffetta et al., 2004).
56 However, most of these studies suffer from a lack of accurate exposure data or even personalized lung-
57 deposited dose information (Peters, Ruckerl, & Cyrus, 2011).

58 Improved exposure studies are under way, but it is still unclear which of the possible dose metrics is
59 best suited for predicting the adverse health outcome of NP exposure. While most (ambient)
60 epidemiological studies were based on mass as the dose metric, there are also a few short-term
61 epidemiological studies indicating that early, transient exacerbations are associated with the number
62 concentration of ultrafine ambient particles rather than the mass of ambient PM (Peters et al., 2011). In
63 toxicology, mass has been used as the dose metric, since mass is the biologically effective dose metric
64 for soluble toxins. However, for non-soluble (or poorly-soluble) soot or engineered NPs only the
65 molecules at the surface of the NPs are interacting with the biological fluids and tissue. Hence, for

66 (nano-)particles surface area is likely to be a biologically more relevant dose metric than mass. This was
67 confirmed by numerous cell-based *in vitro* and animal-based *in vivo* toxicity studies (Oberdörster,
68 Oberdörster, & Oberdörster, 2005; T. Stoeger, Schmid, Takenaka, & Schulz, 2007; Tobias Stoeger et al.,
69 2009; Waters et al., 2009). However, some toxicological studies have also suggested particle number or
70 volume as the most relevant dose metric for NPs (Donaldson et al., 2013; Pauluhn, 2011).

71 State-of-the art aerosol technologies for real-time measurement of all moments of the size distribution
72 (number, length, surface area, volume/mass) of compact aerosols are available (Kulkarni, Baron, &
73 Willeke, 2011). Moreover, the number, joint length, surface area and volume/mass of loosely
74 agglomerated NPs (“soot-like” agglomerates/aggregates) can be determined in real-time by multi-
75 instrument approaches (Wang et al., 2010). For non-hygroscopic, compact NPs (< 300 nm) the lung-
76 deposited surface area concentration can be monitored directly in real-time by electrometer based
77 measurement techniques (Fissan, Neumann, Trampe, Pui, & Shin, 2007). However, for optimized design
78 of future aerosol exposure measurements related to workplace safety or other health-related issues, it
79 is important to identify the biologically most effective dose metric.

80 In this retrospective analysis of selected animal studies on acute pulmonary toxicity of intratracheally
81 instilled NPs we provide guidance on the biologically most relevant dose metric for acute lung
82 inflammation. We investigated the correlation between acute pulmonary inflammation as evidenced by
83 the influx of inflammatory cells into the lung and pulmonary (primary particle) number, joint length,
84 (BET and geometric) surface area, volume and mass as dose metrics. Published data were compiled from
85 nine different studies conducted by various laboratories using different animal models (mouse, rat). The
86 data cover some of the most commonly used types of NPs (polystyrene, titanium dioxide, various
87 carbonaceous materials including aged Diesel soot, quartz, and transition metal oxides) covering a wide
88 range of primary particle diameters (9-535 nm) and mass-specific BET surface areas (6-800 m²/g).

89 Retrospective analysis of this unified data set provides insight into the relevance of the various dose
90 metrics for predicting NP-induced pulmonary toxicity.

91 **2. Materials and methods**

92 The study presented here is based on animal studies on acute pulmonary toxicity due to intratracheal
93 instillation of NPs into the lung. About 60 animal studies on acute pulmonary toxicity published between
94 2001 and 2009 were screened and nine of them were selected for matching all of the following criteria:

- 95 1. Use of mouse or rat as animal models
- 96 2. Particles were applied to the lungs via intratracheal instillation
- 97 3. Data on the influx of polymorphonuclear cells (PMNs) into the lung as hallmark of inflammation
98 are available for at least one (acute) time point (between 16h and 24h after particle application).
99 The number of PMNs and the total number of cells on the lung epithelium was performed via
100 differential cell counting of the bronchoalveolar lavage (BAL) fluid.
- 101 4. Non- or poorly-soluble, smooth, nano-sized (<535 nm) primary particles of spherical shape were
102 used. The state of agglomeration in the applied NP suspension is typically not reported and
103 therefore not considered as criterion here.
- 104 5. Lung-deposited (instilled) mass dose, mass-specific BET surface area and material density are
105 reported (or available).
- 106 6. Accurate information on the primary particle diameter is provided for conversion of the
107 pulmonary mass dose into other dose metrics, namely number, (joint) length, geometric surface
108 area.

109 As mouse and rat are the most frequently used animal models for particle toxicity studies, we included
110 both rat and mouse data here. NPs were delivered to the lungs via intratracheal instillation, i.e. the

111 anesthetized animals were intratracheally intubated and a defined volume of a NP suspension was
112 squirted directly into the lungs with a syringe via the trachea. While this route of application is
113 physiologically not realistic (not an aerosol, but a liquid bolus of a NP suspension is applied), the method
114 is technologically simple, widely used and delivers an accurate and reproducible dose of NPs to the lungs
115 of animals. To account for the large difference in body weight of mice and rats the applied NP doses
116 were allometrically scaled. As we are focusing on pulmonary effects we chose the lung weight as
117 allometric scaling factor. For 7-12 weeks old adult mice lung weights between 0.14 and 0.25 g with an
118 average of about 0.18 g were observed for various strains (Kida, Fujino, & Thurlbeck, 1989). For rats an
119 average value of 1.3 g was reported for the frequently used Fischer F344 rats (1.1-1.5 g; male, 7-20
120 weeks old; (Tillery & Lehnert, 1986)). The choice of 1.3 g and 0.18 g of lung weight for rats and mice,
121 respectively, is also consistent with the widely used allometric dose scaling based on body surface area
122 (Reagan-Shaw, Nihal, & Ahmad, 2008).

123

124 Pulmonary inflammation was chosen as toxicological endpoint, since this represents one of the most
125 sensitive cellular responses and is also considered one of the key adverse effects induced by particulate
126 air pollution (Donaldson, Mills, Macnee, Robinson, & Newby, 2005). One of the hallmarks of pulmonary
127 inflammation is the influx of polymorphonuclear cells (PMNs), such as neutrophils (Henderson, 2005),
128 into the lung which can be determined by bronchoalveolar lavage (BAL) of the lung (rinsing the epithelial
129 surface of the lung with saline solution) and subsequent counting of the number of PMNs in the
130 recovered BAL fluid. Species-, strain- and handling-specific differences in the total number of PMNs
131 retrieved from the lungs are accounted for by normalizing the number of PMNs to the total number of
132 cells in the BAL fluid. As PMN influx into the lung is a time dependent process with a maximum response

133 typically around 24h only data obtained between 16 and 24 h after NP application were included in this
134 study.

135 The pulmonary particle dose was assumed to be the nominal dose, i.e. it was derived from the
136 concentration and the nominally applied volume of the NP suspension. This is an approximation, since a
137 fraction of the nominal dose will remain in the instillation wear. In our laboratory only ca. 85±10% of
138 nominal dose is delivered to the lung (Barapatre et al., 2015) and another ca. 15±10% of nominal dose
139 will be cleared from the (murine) lungs within 24h (van Rijt et al., 2015). Hence, it can be assumed that
140 24h after intratracheal instillation only about 70% of the nominal dose was retained in the lung. This
141 systematic (negative) dose bias of about 30% with an uncertainty of about ±15% was neglected, since it
142 is expected to be similar for instillation-studies and it is much smaller than the about ±2.2-fold dose
143 variability within a given toxicity class of particles (see below).

144 Only materials with low or poor solubility in aqueous media were included, since biopersistent particles
145 were the focus of the present study. Moreover, for calculation of the various dose metrics, namely
146 number (of primary NPs), joint length, geometric and BET surface area as well as volume and mass of
147 the applied NPs, only studies providing the following information were included: diameter of the
148 (spherical) primary NPs (d_p), material density, applied total NP mass (M) and mass-specific BET surface
149 area (SA_{BET}), i.e. the surface area per mass according to the gas adsorption method described by
150 Brunauer, Emmet and Teller (Brunauer, Emmet, & Teller, 1938).

151 From this information the primary particle number (N_p), joint length (L_p) and geometric surface area
152 (SA_{geom}) of the applied NPs was calculated according to

153
$$N_p = \frac{M}{\rho_p \left(\frac{\pi d_p^3}{6} \right)}, \quad L_p = N_p d_p, \quad \text{and} \quad SA_{geom} = N_p \pi d_p^2, \quad (1)$$

154 respectively, where M and ρ_p represent the applied NP mass and the material density, respectively.
155 Moreover, the BET surface area dose SA_{BET} was calculated from

$$156 \quad SA_{BET} = sa_{BET} M, \quad (2)$$

157 where sa_{BET} is the mass-specific BET surface area (m^2/g). The volume dose V is given by

$$158 \quad V = \frac{M}{\rho_p f}, \quad (3a)$$

159 where $f = 0.74$ is the volume filling fraction of closely packed spheres, which accounts for the void
160 spaces between the primary particles. The assumption of a close packed structure is justified by the
161 toxicological mode of action related to volume as dose metric. As discussed in more detail below for
162 chronic exposures, if the volume of NPs, which are taken up (phagocytized) by alveolar macrophages,
163 exceeds a limiting (overload) dose, PMN release into the lung is observed (Pauluhn, 2011). It has been
164 shown that even loosely packed NP agglomerates are strongly compacted inside macrophages justifying
165 the assumption of a close packed NP structure for estimating the effective volume dose (Takenaka et al.,
166 2012). For interpretation of the volume data with respect to the so-called overload conditions, it is
167 important to normalize the phagocytized NP volume to the total volume of the alveolar macrophages in
168 the lung, which is given by equation 3b for rats (Pauluhn, 2011)

$$169 \quad V_{alv,mac} = 7 \times 10^{10} \mu m^3 / kg. \quad (\text{for rats}) \quad (3b)$$

170 This equation can be allometrically scaled for mice

$$171 \quad V_{alv,mac} = 7 \times 10^{10} \mu m^3 / kg \times 0.3 kg \frac{0.18 g}{1.3 g}, \quad (\text{for mice}) \quad (3c)$$

172 based on lung and body weight as justified above (assumed body weight for rat/mouse: 300 g/20 g;
173 lung weight: 1.3 g/0.18 g).

174

175 **Results**

176 In this comparative study *in vivo* animal data from our laboratory (T. Stoeger et al., 2006) and from eight
177 other studies were combined to investigate acute pulmonary inflammation for five different material
178 types, a wide range of primary particles in the nano-size range (diameter: 9-535 nm), mass-specific BET
179 surface areas (6-800 m²/g) and dose range (several orders of magnitude) (see Table 1). The five
180 different types of biopersistent materials comprise polystyrene, two types of titanium dioxide (TiO₂), six
181 types of carbonaceous materials (including flame soot, Diesel soot and carbon black (Printex90)) as well
182 as transition metal oxides (Co-, Ni-, and Zn-oxides) and hydrolyzed α -quartz (α -crystalline silica, SiO₂). A
183 total number of 58 data points were included in this study.

184 High quality of the allometric dose scaling approach used here is a prerequisite for combining rat and
185 mouse data in this retrospective-analysis. This issue was examined using the five TiO₂ data sets for mice
186 (1) and rats (4) obtained in different laboratories (see Table 1). As seen from Figure 1A there is excellent
187 agreement between the dose-response curves from all five data sets. The logarithmic fit of PMN number
188 versus BET surface area dose explains 91% of the variability of the toxicological response ($R^2=0.91$).
189 Hence, normalizing the pulmonary particle dose to the lung weight allows comparison of (normalized)
190 PMN data from rats and mice on the same dose-scale. Moreover, Figure 1A also shows great
191 consistence of data from different laboratories which is another prerequisite for reliable retrospective-
192 analysis of data from different laboratories.

193 The dose-response data presented in Figures 1 and 2 show a sigmoidal shape with a no observed effect
194 level (NOEL) between 0 and 5% (no inflammation) for low doses and an asymptotic maximum response
195 level between 50 and 70% (maximum (100%) observed effect level (MOEL)) for high doses. As both the
196 asymptotic NOEL and MOEL are not far enough explored for sigmoidal curve fitting, we performed
197 logarithmic dose-response fits over the entire data set and compared particle-specific toxicities based
198 on EC_{50} values, i.e. effect concentration/dose at 50% of MOEL (= 30% PMN) as seen in Figure 1B. As the
199 fit is not valid for PMN values below 5% and above 60%, the fit curves are truncated at these PMN
200 values.

201 Figure 1B depicts acute pulmonary inflammation induced by four different types of materials with
202 similar toxicological classification, namely polystyrene, TiO_2 , (six types of) carbonaceous materials and
203 hydrolyzed nano-quartz (Table 1). Again there is good linear correlation between (logarithmic) dose and
204 toxicological response ($R^2=0.76$) for BET surface area as the dose metric. The derived EC_{50} dose
205 corresponds to a (geometric) mean dose of $175 \text{ cm}^2/\text{g-lung}$. Moreover, all data are clustering relatively
206 tightly about the dose-response fit curve resulting in EC_{50} dose variability from 85 to $405 \text{ cm}^2/\text{g-lung}$
207 ($\pm 1\sigma$ dose limits). This dose range corresponds to a moderate geometric standard deviation of 2.2
208 ($= (405/85)^{0.5}$) about the mean, which is similar to the width of typically observed aerosol size
209 distributions such as produced by standard aerosol generators. Consequently, the four types of
210 materials presented in Figure 1B can be categorized as a specific toxicity class sometimes referred to
211 as *low-solubility, low-toxicity* (LSLT) materials without intrinsic toxicity.

212

213 Figure 2 compares the toxicity of transition metal oxides (cobalt (Co), nickel (Ni), zinc (Zn)) to that of
214 LSLT materials. As seen in Figure 2A the EC_{50} dose for the investigated transition metal oxides is
215 $15 \text{ cm}^2/\text{g-lung}$ indicating that cobalt, nickel and zinc oxide show 12-fold higher BET surface-specific

216 toxicity than LSLT particles ($EC_{50} = 175 \text{ cm}^2/\text{g-lung}$). Virtually the same result is found for geometric
217 (instead of BET) surface area as dose metric with the limitation that only two of the six BET-based
218 transition metal data points could be converted into geometric volume due to a lack of particle-specific
219 information (see Table 1). In light of the wide range of primary particle diameters (9-535 nm), the
220 absence of any significant size-dependent particle toxicity is remarkable and documents the biological
221 relevance of surface area as dose metric.

222 In addition to surface area other dose metrics were investigated. Figure 3 shows the same data as
223 depicted in Figure 2, but presented in terms of number, joint length, volume and mass. Using mass and
224 volume as the dose metric shows a correlation coefficients of $R^2 = 0.49$ and 0.52 , respectively (Figure 3A
225 and 3B), which is significantly lower than the 0.76 (or 0.78) for BET and geometric surface area,
226 respectively (Figure 2). Moreover, the higher toxicity of transition metals compared to LSLT materials is
227 not evident for mass and volume as the dose metric. Expressing the dose-response curves in terms of
228 number and joint length of the primary NPs (only LSLT particles were considered), yields even lower
229 dose-response correlation coefficients of 0.19 and 0.41 , respectively (see Figure 3C and 3D). The
230 relatively high correlation coefficient of joint length compared to number concentration in spite of very
231 similar scatter plots is a result of the fact that the relative x-axis range is much narrower for length than
232 for number (ca. 3 and 5 orders of magnitude, respectively). However, both metrics display a size-
233 dependent stratification of the data, with larger primary particle diameters inducing larger PMN influx.
234 However, this is an artefact due to the larger surface area per particle for larger sizes. Hence neither
235 number nor joint length is a suitable dose metric for LSLT particles.

236 **Discussion**

237 The retrospective-analysis presented here identifies surface area as the biologically most relevant dose
238 metric for non- or low-solubility NPs of spherical shape. However, this analysis is based on non-

239 physiologically applied NPs using intratracheal instillation instead of inhalation. Naturally, inhalation
240 studies are considered the gold standard for inhalation risk assessment. Hence, it is important to
241 compare our findings to results from inhalation studies. Numerous chronic (>14 weeks of exposure),
242 sub-chronic (1-14 weeks) and acute (<1 weeks) animal inhalation studies are also providing evidence for
243 surface area as the biologically most relevant dose metric for non-soluble particles. For instance, the
244 lung tumor prevalence occurring in animal models after chronic inhalation of toner, coal dust, talc,
245 titanium dioxide, diesel soot and carbon black particles was found to be well correlated with pulmonary
246 surface area dose (Maynard & Kuempel, 2005). Another retrospective-analysis of animal data on the
247 carcinogenicity of inhaled particles found elevated toxicity of particles smaller than 100 nm for mass as
248 dose metric, but no size-dependence for surface area or volume dose (Gebel, 2012). Also short-term
249 inhalation studies with different sized silver NPs implied surface area as the biologically most relevant
250 dose metric for acute pulmonary inflammation (Braakhuis et al., 2015). Surface area as biologically most
251 relevant dose metric may be rationalized by the fact that only molecules on the particle surface area are
252 in direct contact with bodily fluids and tissue. Hence, effects such as attachment of a protein corona or
253 formation of reactive oxygen species and subsequent adverse effects on cell homeostasis are likely to
254 depend on particle surface area dose (Fubini, Ghiazza, & Fenoglio, 2010; Tobias Stoeger et al., 2009; Xia
255 et al., 2006).

256 However, there are also inhalation studies championing volume as biologically most relevant dose
257 metric. In a retrospective-analysis of sub-chronic inhalation studies (4-13 weeks exposure) with a wide
258 variety of particle types (e.g. AlOOH, Fe₂O₃, TiO₂, multi-walled carbon nanotubes – in entangled,
259 agglomerated form), it was shown that PMN influx in the lung was best correlated with the volume
260 burden of the particles in the lung (Pauluhn, 2009, 2011). The dose-response curves were consistent
261 with the well-known overload paradigm of particle toxicity, which claims that particles without inherent
262 toxicity are non-toxic in chronic inhalation scenarios unless the pulmonary particle volume burden

263 exceeds 6% of the macrophage volume of the lung (Pauluhn, 2011). Once this dose threshold, known as
264 the overload condition, is reached the mobility of alveolar macrophages and their ability of clearing
265 particles from the alveolar air space is retarded leading to chronic inflammation and associated adverse
266 health effects (Pauluhn, 2011).

267 In addition to surface area and volume, particle number has been identified as biologically effective dose
268 metric for stiff, biopersistent, fiber-like particles such as asbestos or other fiber-like particles. While
269 short fiber-like particles can be phagocytized,) fiber-like particles longer than 5 μm (some say longer
270 than 15-20 μm) are too long for macrophages to completely engulf them. This *frustrated phagocytosis*
271 results in persistent inflammatory stimulation leading to fibrotic or carcinogenic tissue degradation
272 (Archer, 1979; Murphy, Schinwald, Poland, & Donaldson, 2012). As each fiber can eliminate the same
273 number of macrophages, particle number is the biologically most effective dose metric for this mode of
274 action.

275 In light of the large number of engineered nanomaterials being developed, chronic inhalation studies are
276 too time consuming and expensive for rigorous risk assessment. Hence, intratracheal instillation animal
277 studies on acute lung inflammation may serve as cost effective, reliable, early indicator of potential
278 adverse health effects of inhaled particles. Figure 1A confirms that both inter-species (mouse and rat)
279 and inter-laboratory variability is sufficiently small to obtain consistent data sets. In the present
280 retrospective-analysis we investigated the moments of the particle size distribution (0th, 1st, 2nd and 3rd
281 moment correspond to the mean number, length, surface area, volume/mass of the particle size
282 distribution) for their biological relevance for acute lung inflammation in animal models.

283 Clearly, primary particle number and joint length proved to be inferior to particle mass and volume
284 (Figure 3). This assessment is not only based on the poor correlation coefficient of number and length,
285 but also on the size-stratification of the data (larger particles appear more toxic), which is most

286 pronounced for number and length as the dose metric, but also present in the volume and mass data
287 (not shown in Figure 3A and 3B), although to a much smaller degree. Historically, most of the particle
288 toxicity studies were performed with mass as the dose metric. While mass is an adequate dose metric
289 for soluble materials, it is inadequate for non- and low-solubility particles used here. In fact using mass
290 as dose metric has led to the false conclusion that smaller particles are inherently more toxic than larger
291 ones (Gebel, 2012). On the other hand, smaller particles appear to be less toxic than larger ones, if
292 number or length is chosen as the dose metric. This apparent dependence of toxicity on particle size
293 vanishes, if surface area is used as the dose metric as shown by our and numerous other studies
294 (Braakhuis et al., 2015).

295 Volume dose displayed similarly mediocre correlation with acute inflammation as mass. For none of the
296 cases investigated here, the overload dose (6% of macrophage volume) was exceeded (Figure 3B).
297 Hence, the observed significant acute inflammatory response for some cases cannot be explained with
298 the overload paradigm. In fact the overload paradigm refers to chronic inflammation and not to acute
299 effects. Hence, this mode of action is not expected to be relevant for the data analyzed here.

300 The retrospective-analysis of acute lung inflammation data indicates that surface area is the biologically
301 most effective dose metric with no significant difference between BET or geometric surface area
302 (Figure 2B), which is consistent with the fact that the materials investigated here had smooth surfaces
303 without significant microporous structures. This can be seen from the ratios of geometric and BET
304 surface area ranging from 0.41 to 1.5 with most of the particles clustering about unity (Table 1). For
305 microporous and non-spherical particle shapes (except fibers) BET rather than geometric surface area is
306 expected to be the biologically more effective (or more easily determined) dose metric. In contrast to
307 geometric surface area, there is currently no real-time measurement method for BET surface area. Thus,
308 the fact that for spherical particles with smooth surfaces the geometric surface area can be used as

309 biologically most relevant dose metric has severe practical implications for exposure measurements.
310 Using recently described multi-instrument approaches it is possible to determine all moments (0th to 3rd
311 moment) of nanoparticle size distributions for both spherical and agglomerated (smooth) spherical NPs
312 as required for nanoparticle inhalation risk assessment (Shin et al., 2010; Wang et al., 2010).

313 The close proximity of the dose-response curves of the four different types of LSLT materials
314 (polystyrene, TiO₂, carbonaceous materials, smooth quartz) depicted in Figure 2 indicates that these
315 materials have similar surface-specific toxicity possibly due to similar catalytic activity of the surface.
316 These types of materials are considered materials without intrinsic toxicity. On the other hand, it is well
317 known that certain transition metal oxides and milled quartz have enhanced toxicity. Figure 2 shows
318 evidence for 12-fold enhanced surface-specific toxicity of Co-, Ni- and Zn-oxide compared to LSLT
319 materials. This can be attributed to the production of highly toxic free OH-radicals from hydrogen
320 peroxide (Fenton reaction) and uptake of particles in intracellular compartments (the endo-lysosomal
321 system) with low pH, where partial dissolution leads to the release of high (toxic) concentrations of
322 metal ions in the cells. This so-called Trojan horse effect can also lead to an imbalance of the
323 intracellular homeostasis of otherwise tightly regulated metal ions and subsequent inflammatory
324 response. These additional modes of action account for the enhanced surface-specific toxicity of
325 transition metal compared to LSLT NPs. Our study also shows that synthesized, nano-sized α -crystalline
326 silica (α -quartz) belongs to the LSLT toxicity class (Figure 2). This may seem surprising as numerous
327 studies report elevated surface-specific toxicity for quartz particles such as Min-U-Sil (Warheit, Webb,
328 Colvin, Reed, & Sayes, 2007), which was not included here because of its super-micron size and irregular
329 particle shape. For grinded quartz (like Min-U-Sil), it has been hypothesized that the sharp-edged
330 particles can cause lysosomal membrane destabilization, which contributes to the elevated
331 inflammatory toxicity (Sun, Wang, Ji, Li, & Xia, 2013). As the hydrothermally synthesized nano-quartz
332 used by Warheit and coworkers has smooth surface structure (Warheit et al., 2007) lysosomal

333 destabilization has not been activated, which explains the observed low toxicity levels comparable to
334 LSLT particles.

335 The analysis presented here also indicates that primary particle size has no effect on surface-specific
336 particle toxicity. As caveat we add that this study was not designed to study effects of primary particle
337 size on surface-specific toxicity. Hence, we cannot rule out that size-dependent effects do occur
338 especially for very small primary particle sizes, where quantum effects may come into play. Moreover,
339 many toxicologically relevant modes of action such as endocytic cellular uptake of non-professional
340 phagocytic cells depend on agglomerate rather than primary particle size. The means of application
341 (intratracheal instillation) suggests that rather large agglomerates had formed either in the particle
342 suspension or on the lung epithelium. Thus, we can only conclude that for agglomerated LSLT particles
343 the combined effect of primary particle size and material type on acute lung toxicity is less than a factor
344 of 4.8 ($2\sigma_g$ of EC50; see Figure 1B).

345 For aerosol exposure measurements it is important to note that not surface area concentration, but the
346 toxicologically effective, lung-deposited surface area concentration is expected to be the biologically
347 most effective dose metric for non-soluble NPs. This is evident from equation 4, describing the
348 relationship between the *effective lung-deposited surface area dose* ($Dose_{SAeff}$) and the surface area (or
349 mass) exposure level of the aerosolized nanoparticles

350
$$Dose_{SA,eff} = f_{tox} \dot{V} t \int [m(D)sa(D)Dep(D)]dD , \quad (4)$$

351 where $m(D) = dM/dD$ is the differential particle mass distribution (D = particle diameter), $Dep(D)$ is the
352 size-dependent fraction of inhaled particles deposited onto the lung epithelium (see e.g. (ICRP, 1994;
353 Londahl et al., 2014), sa is the mass-specific surface area of the particles, t is the exposure time and \dot{V} is
354 the ventilation rate of the lung (inhaled air volume per time). To account for different relative toxicities

355 (high and low toxicity class) the toxicological weighting factor f_{tox} is introduced which accounts for
356 differences in surface-specific toxicity, which can be defined as the *inverse* of the normalized surface-
357 based EC_{50} value, where the LSLT EC_{50} value is a suitable normalization constant (i.e. $f_{tox} = 12$ and 1 for
358 transition metal oxide and LSLT nanoparticles having EC_{50} values of 15 and 175 cm^2/g -lung,
359 respectively). If any of the parameters in equation 4 is time-dependent, time averages have to be used
360 or the right hand side of equation 4 has to be integrated over time as well. For long-term exposures,
361 time-dependent particle clearance rates may have to be included as well.

362 The integral term in equation 4 represents the lung-deposited surface area concentration, which –
363 under certain conditions - can be measured in real-time by electrometer-based measurement
364 techniques (e.g. NSAM or AeroTrak by TSI, Partector by Naneos; (Fissan et al., 2007)). These devices
365 provide reliable lung-deposited surface area concentrations for smooth, compact particles with
366 diameters between about 20 and 300 nm, i.e. they do not necessarily adequately account for effects of
367 shape, agglomeration state or surface-porosity on surface area (Wang et al., 2010). These instruments
368 do also not account for hygroscopic particle growth in the lung making the results unreliable for
369 (partially) water-soluble particles. Thus, for non-soluble compact particles only are electrometer-based
370 measurement techniques expected to provide a valuable tool for real-time exposure measurement of
371 the biologically most effective particle dose (lung-deposited surface area dose). Moreover, for
372 agglomerated spherical NPs, multi-instrument approaches can be used for real-time measurement of
373 both primary particle size and particle number which can then be converted into derived surface area
374 (for smooth surfaces) and volume concentration (Shin et al., 2010; Wang et al., 2010). Ultimately, any of
375 these dose metrics can then be converted into lung-deposited dose by accounting for the known size-
376 dependent lung deposition fraction (ICRP, 1994; Londahl et al., 2014).

377 As seen in Figure 2 spherical nanoparticles can be stratified into surface-based classes of. As suggested
378 in equation 4 these differences in surface-specific toxicity can be incorporated into risk assessment by
379 defining appropriate toxicity weighting factors. For instance our retrospective-analysis suggests that
380 transition metal oxides and LSLT particles can be presented by $f_{tox} = 12$ and 1, respectively, based on the
381 ratios of the corresponding EC_{50} values. Recently, there have been attempts of defining equivalent
382 toxicological doses using the concept of lung-deposited surface area and appropriate weighting factors
383 accounting for enhanced health risks due to e.g. highly toxic materials, surface roughness and the
384 occurrence of frustrated phagocytosis (Simko, Nosske, & Kreyling, 2014).

385 As discussed above the EC_{50} doses presented here are expected to provide a valuable tool for comparing
386 the *relative* toxicity of different types of nanoparticles, but they are *not* suitable as sole basis for
387 recommended exposure limits of nanoparticles (*absolute* toxicity). The latter is mainly because exposure
388 limits should be based on chronic inhalation studies rather than on acute instillation studies as
389 presented here. Nevertheless, from the perspective of exposure assessment it is instructive to relate
390 the EC_{50} values derived here to corresponding exposure concentrations. Assuming a worst case
391 exposure scenario, the EC_{50} values of 175 and 15 m^2/g -lung for nanoparticles belonging to the low and
392 high toxicity class defined in Figure 2, respectively, are allometrically equivalent to the lung-deposited
393 surface area dose received by a person during an 8-hour work shift at an aerosol mass concentration of
394 360 and 30 $\mu g/m^3$, respectively. Here, the following worst case assumptions were made: The worker
395 conducted heavy work during the entire 8 hour shift (3 m^3/h ventilation rate, (ICRP, 1994), the lung
396 deposited aerosol fraction in the alveoli is 60% (ICRP, 1994) and the mass-specific surface area of the
397 nanoparticles is 1000 m^2/g . Allometric scaling of the lung deposited particle dose from mouse/rat to
398 man was based on an assumed lung surface area of 100 m^2 and 600 cm^2 (for a 0.18 g mouse lung) for
399 man and mouse, respectively (Kida et al., 1989; Paur et al., 2011; K. C. Stone, Mercer, Gehr, Stockstill, &
400 Crapo, 1992). Thus, the EC_{50} doses of 175 and 15 m^2/g -lung can be converted into corresponding EC_{50}

401 doses normalized to lung surface area of 530 and 45 cm²/m²-lung, respectively. We reiterate that these
402 exposure levels should not be interpreted as guidance for NP workplace exposure limits, because of the
403 difficulties of relating acute pulmonary effects observed after instillation of NP into the lung to adverse
404 health effects due to chronic inhalation scenarios.

405

406 **Conclusions**

407 The retrospective-analysis provided here showed that allometrically scaled animal data from mice and
408 rats provide species- and laboratory-independent information on the pulmonary toxicity of
409 intratracheally instilled nanoparticles (NPs). For low- and poorly-soluble spherical NPs, (lung-deposited)
410 particle surface area emerged as the biologically most effective dose metric for predicting acute
411 pulmonary inflammation. As expected, there was no significant difference between BET and geometric
412 surface area as dose metric for relatively nanoparticles with smooth surface structure (no micro-pores).

413 Using surface area as the dose metric allowed identification of size-independent toxicity classes.

414 Materials with no intrinsic toxicity like polystyrene, carbonaceous materials, titanium dioxide and
415 synthesized (smooth) α -quartz (but not Min-U-Sil quartz) showed similar dose response curves
416 clustering in a narrow dose range between 85 and 405 m²/g-lung (geometric mean at 175 m²/g-lung;
417 geometric standard deviation of 2.2) at half-maximum response level (EC_{50}) corresponding to 30% PMN
418 influx into the lungs. This toxicity class was referred to as low solubility, low toxicity (LSLT) class. It is
419 noteworthy that not only (aged) diesel soot, but also all other five types of carbonaceous materials
420 considered here belong to the LSLT class suggesting that also ambient urban ultrafine particles might
421 belong to the LSLT class at least in the absence of highly toxic material adsorbed onto the core of these
422 particles. For transition metal oxides (here: Co, Ni, Zn), which are considered materials with intrinsic

423 toxicity, a surface-specific toxicity enhancement factor of about 12 compared to LSLTS particles was
424 found ($EC_{50} = 15 \text{ m}^2/\text{g-lung}$).

425 As caveat we add that applying NP suspensions rather than freshly generated aerosols may have an
426 effect on the observed surface-specific toxicity due to interactions of the liquid with the particles.
427 However, the notion that surface area is the most relevant dose metric for particle toxicity has also been
428 shown by numerous inhalation studies. Depending on the mode of action, dose metrics other than
429 surface area may be more effective. For instance, volume and number are biologically more effective
430 dose metrics for high particle lung burden (overload conditions; more than 6% of alveolar macrophage
431 volume is filled with particles) and long, stiff fiber-like particles (frustrated phagocytosis).

432 With these limitations in mind lung-deposited particle surface area dose can be expected to be the
433 toxicologically most relevant dose metric for inhaled NPs. Hence, future aerosol exposure
434 measurements related to health effects of inhaled particles should strive to include lung-deposited
435 particle surface area concentration as the main exposure parameter. Moreover, particle number and
436 volume should be measured especially for high aspect ratio particles and high pulmonary particle doses,
437 respectively, and even mass should be included, since mass has been the historically used as dose metric
438 for substance toxicity.

439

440 **Literature**

441 Archer, V. E. (1979). Carcinogenicity of fibers and films: a theory. *Med Hypotheses*, 5(11), 1257-1262.
442 Barapatre, N., Symvoulidis, P., Möller, W., Prade, F., Deliolanis, N. C., Hertel, S., . . . Schmid, O. (2015).
443 Quantitative detection of drug dose and spatial distribution in the lung revealed by Cryoslicing
444 Imaging. *Journal of Pharmaceutical and Biomedical Analysis*, 102, 129-136.
445 Boffetta, P., Soutar, A., Cherrie, J. W., Granath, F., Andersen, A., Anttila, A., . . . Weiderpass, E. (2004).
446 Mortality among workers employed in the titanium dioxide production industry in Europe.
447 *Cancer Causes Control*, 15(7), 697-706. doi: 10.1023/B:CACO.0000036188.23970.22

448 Braakhuis, H. M., Cassee, F. R., Fokkens, P. H. B., de la Fonteyne, L. J. J., Oomen, A. G., Krystek, P., . . .
449 Park, M. V. D. Z. (2015). Identification of the appropriate dose metric for pulmonary
450 inflammation of silver nanoparticles in an inhalation toxicity study. *Nanotoxicology, Early Online:*
451 *1–11*, DOI: 10.3109/17435390.17432015.11012184.

452 Brown, D. M., Wilson, M. R., MacNee, W., Stone, V., & Donaldson, K. (2001). Size-dependent
453 proinflammatory effects of ultrafine polystyrene particles: A role for surface area and oxidative
454 stress in the enhanced activity of ultrafines. *Toxicology and Applied Pharmacology, 175*(3), 191-
455 199.

456 Brunauer, S., Emmet, P. H., & Teller, E. (1938). Adsorption of gases in multimolecular layers. *Journal of*
457 *the American Chemical Society, 60*, 309-319.

458 Dick, C. A., Brown, D. M., Donaldson, K., & Stone, V. (2003). The role of free radicals in the toxic and
459 inflammatory effects of four different ultrafine particle types. *Inhal Toxicol, 15*(1), 39-52. doi:
460 10.1080/08958370304454

461 Donaldson, K., Mills, N., Macnee, W., Robinson, S., & Newby, D. (2005). Role of inflammation in
462 cardiopulmonary health effects of PM. *Toxicol Appl Pharmacol, 207*(2 Suppl), 483-488.

463 Donaldson, K., Schinwald, A., Murphy, F., Cho, W. S., Duffin, R., Tran, L., & Poland, C. (2013). The
464 Biologically Effective Dose in Inhalation Nanotoxicology. *Accounts of Chemical Research, 46*(3),
465 723-732.

466 Fissan, H., Neumann, S., Trampe, A., Pui, D. Y. H., & Shin, W. G. (2007). Rationale and Principle of an
467 Instrument Measuring Lung Deposited Nanoparticle Surface Area. *Journal of Nanoparticle*
468 *Research, 9*, 53-59.

469 Fubini, B., Ghiazza, M., & Fenoglio, I. (2010). Physico-chemical features of engineered nanoparticles
470 relevant to their toxicity. *Nanotoxicology, 4*(4), 347-363.

471 Gebel, T. (2012). Small difference in carcinogenic potency between GBP nanomaterials and GBP
472 micromaterials. *Archives of Toxicology, 86*(7), 995-1007.

473 Henderson, R. F. (2005). Use of bronchoalveolar lavage to detect respiratory tract toxicity of inhaled
474 material. *Exp Toxicol Pathol, 57 Suppl 1*, 155-159.

475 Hohr, D., Steinfartz, Y., Schins, R. P., Knaapen, A. M., Martra, G., Fubini, B., & Borm, P. J. (2002). The
476 surface area rather than the surface coating determines the acute inflammatory response after
477 instillation of fine and ultrafine TiO₂ in the rat. *Int J Hyg Environ Health, 205*(3), 239-244.

478 ICRP. (1994). International Commission on Radiological Protection (ICRP), Human respiratory tract
479 model for radiological protection: a report of a task group of the ICRP *ICRP publication 66;*
480 *Annals of the ICRP* (Vol. 24, pp. 1-482). Oxford, UK: Elsevier Science Ltd.

481 Kida, K., Fujino, Y., & Thurlbeck, W. M. (1989). A comparison of lung structure in male DBA and C57 black
482 mice and their F1 offspring. *Am Rev Respir Dis, 139*(5), 1238-1243.

483 Kulkarni, P., Baron, P. A., & Willeke, K. (2011). *Aerosol Measurement: Principles, Techniques, and*
484 *Applications*. New York: John Wiley and Sons.

485 Londahl, J., Moller, W., Pagels, J. H., Kreyling, W. G., Swietlicki, E., & Schmid, O. (2014). Measurement
486 Techniques for Respiratory Tract Deposition of Airborne Nanoparticles: A Critical Review.
487 *Journal of Aerosol Medicine and Pulmonary Drug Delivery, 27*(4), 229-254. doi: DOI
488 10.1089/jamp.2013.1044

489 Lu, S. L., Duffin, R., Poland, C., Daly, P., Murphy, F., Drost, E., . . . Donaldson, K. (2009). Efficacy of Simple
490 Short-Term in Vitro Assays for Predicting the Potential of Metal Oxide Nanoparticles to Cause
491 Pulmonary Inflammation. *Environmental Health Perspectives, 117*(2), 241-247.

492 Maynard, A. D., & Kuempel, E. D. (2005). Airborne nanostructured particles and occupational health.
493 *Journal of Nanoparticle Research, 7*(6), 587-614.

494 Murphy, F. A., Schinwald, A., Poland, C. A., & Donaldson, K. (2012). The mechanism of pleural
495 inflammation by long carbon nanotubes: interaction of long fibres with macrophages stimulates

496 them to amplify pro-inflammatory responses in mesothelial cells. *Part Fibre Toxicol*, 9, 8. doi:
497 10.1186/1743-8977-9-8

498 Oberdörster, G., Oberdörster, E., & Oberdörster, J. (2005). Nanotoxicology: An emerging discipline
499 evolving from studies of ultrafine particles. *Environmental Health Perspectives*, 113(7), 823-839.

500 Pauluhn, J. (2009). Retrospective analysis of 4-week inhalation studies in rats with focus on fate and
501 pulmonary toxicity of two nanosized aluminum oxyhydroxides (boehmite) and pigment-grade
502 iron oxide (magnetite): The key metric of dose is particle mass and not particle surface area.
503 *Toxicology*, 259(3), 140-148.

504 Pauluhn, J. (2011). Poorly soluble particulates: Searching for a unifying denominator of nanoparticles
505 and fine particles for DNEL estimation. *Toxicology*, 279(1-3), 176-188.

506 Paur, H.-R., Cassee, F. R., Teeguarden, J., Fissan, H., Diabate, S., Aufderheide, M., . . . Schmid, O. (2011).
507 In-vitro cell exposure studies for the assessment of nanoparticle toxicity in the lung—A dialog
508 between aerosol science and biology. *Journal of Aerosol Science*, 42, 668–692.

509 Peters, A., Ruckerl, R., & Cyrys, J. (2011). Lessons From Air Pollution Epidemiology for Studies of
510 Engineered Nanomaterials. *Journal of Occupational and Environmental Medicine*, 53(6), S8-S13.

511 Reagan-Shaw, S., Nihal, M., & Ahmad, N. (2008). Dose translation from animal to human studies
512 revisited. *Faseb Journal*, 22(3), 659-661. doi: DOI 10.1096/fj.07-9574LSF

513 Salvi, S. (2007). Health effects of ambient air pollution in children. *Paediatr Respir Rev*, 8(4), 275-280.
514 doi: 10.1016/j.prrv.2007.08.008

515 Sayes, C. M., Reed, K. L., & Warheit, D. B. (2007). Assessing toxicity of fine and nanoparticles: Comparing
516 in vitro measurements to in vivo pulmonary toxicity profiles. *Toxicological Sciences*, 97(1), 163-
517 180.

518 Shin, W. G., Wang, J., Mertler, M., Sachweh, B., Fissan, H., & Pui, D. Y. H. (2010). The effect of particle
519 morphology on unipolar diffusion charging of nanoparticle agglomerates in the transition
520 regime. *Journal of Aerosol Science*, 41(11), 975-986. doi: DOI 10.1016/j.jaerosci.2010.07.004

521 Simko, M., Nosske, D., & Kreyling, W. G. (2014). Metrics, dose, and dose concept: the need for a proper
522 dose concept in the risk assessment of nanoparticles. *Int J Environ Res Public Health*, 11(4),
523 4026-4048. doi: 10.3390/ijerph110404026

524 Stoeger, T., Reinhard, C., Takenaka, S., Schroepfel, A., Karg, E., Ritter, B., . . . Schulz, H. (2006).
525 Instillation of six different ultrafine carbon particles indicates a surface area threshold dose for
526 acute lung inflammation in mice. *Environmental Health Perspectives*, 114(3), 328-332.

527 Stoeger, T., Schmid, O., Takenaka, S., & Schulz, H. (2007). Inflammatory response to TiO₂ and
528 Carbonaceous particles scales best with BET surface area. *Environmental Health Perspectives*,
529 115(6), A290-A291.

530 Stoeger, T., Takenaka, S., Frankenberger, B., Ritter, B., Karg, E., Maier, K., . . . Schmid, O. (2009).
531 Deducing in vivo toxicity of combustion-derived nanoparticles from a cell-free oxidative potency
532 assay and metabolic activation of organic compounds. *Environmental Health Perspectives*,
533 117(1), 54-60.

534 Stone, K. C., Mercer, R. R., Gehr, P., Stockstill, B., & Crapo, J. D. (1992). Allometric relationships of cell
535 numbers and size in the mammalian lung. *Am J Respir Cell Mol Biol*, 6(2), 235-243.

536 Stone, V., Johnston, H., & Clift, M. J. (2007). Air pollution, ultrafine and nanoparticle toxicology: cellular
537 and molecular interactions. *IEEE Trans Nanobioscience*, 6(4), 331-340.

538 Sun, B., Wang, X., Ji, Z., Li, R., & Xia, T. (2013). NLRP3 inflammasome activation induced by engineered
539 nanomaterials. *Small*, 9(9-10), 1595-1607. doi: 10.1002/smll.201201962

540 Takenaka, S., Moller, W., Semmler-Behnke, M., Karg, E., Wenk, A., Schmid, O., . . . Kreyling, W. G. (2012).
541 Efficient internalization and intracellular translocation of inhaled gold nanoparticles in rat
542 alveolar macrophages. *Nanomedicine (Lond)*, 7(6), 855–865. doi: 10.2217/nnm.11.152

543 Tillery, S. I., & Lehnert, B. E. (1986). Age-bodyweight relationships to lung growth in the F344 rat as
544 indexed by lung weight measurements. *Lab Anim*, 20(3), 189-194.

545 van Rijt, S. H., Bölükbas, D. A., Argyo, C., Wipplinger, K., Naureen, M., Datz, S., . . . Stoeger, T. (2015).
546 Bioresponse of avidin protein coated mesoporous silica nanoparticles in the lung. *Biomaterials*,
547 submitted

548 Wang, J., Shin, W. G., Mertler, M., Sachweh, B., Fissan, H., & Pui, D. Y. H. (2010). Measurement of
549 Nanoparticle Agglomerates by Combined Measurement of Electrical Mobility and Unipolar
550 Charging Properties. *Aerosol Science and Technology*, 44(2), 97-108.

551 Warheit, D. B., Webb, T. R., Colvin, V. L., Reed, K. L., & Sayes, C. R. (2007). Pulmonary bioassay studies
552 with nanoscale and fine-quartz particles in rats: Toxicity is not dependent upon particle size but
553 on surface characteristics. *Toxicological Sciences*, 95(1), 270-280. doi: DOI 10.1093/toxsci/kfl128

554 Warheit, D. B., Webb, T. R., Sayes, C. M., Colvin, V. L., & Reed, K. L. (2006). Pulmonary instillation studies
555 with nanoscale TiO₂ rods and dots in rats: Toxicity is not dependent upon particle size and
556 surface area. *Toxicological Sciences*, 91(1), 227-236.

557 Waters, K. M., Masiello, L. M., Zangar, R. C., Tarasevich, B. J., Karin, N. J., Quesenberry, R. D., . . . Thrall,
558 B. D. (2009). Macrophage responses to silica nanoparticles are highly conserved across particle
559 sizes. *Toxicol Sci*, 107(2), 553-569. doi: 10.1093/toxsci/kfn250

560 Xia, T., Kovochich, M., Brant, J., Hotze, M., Sempf, J., Oberley, T., . . . Nel, A. E. (2006). Comparison of the
561 Abilities of Ambient and Manufactured Nanoparticles To Induce Cellular Toxicity According to an
562 Oxidative Stress Paradigm. *Nano Letters*, 6(8), doi:10.1021/nl061025k, 061794-061807.

563

564

565 **Table 1** Physico-chemical characteristics of the different types of (agglomerated) nanoparticles (NPs)
 566 included in the retrospective study presented here. Particles were applied directly into the lungs of mice
 567 and rats via intratracheal instillation (i.e. as liquid bolus not as aerosol).

Type	Material (Nanoparticles)			Ratio Geometric/BET Surface Area	Dose Mass Dose per Animal (mg)	Animal Species	Reference
	Primary Diameter (nm)	Density (g/cm ³)	Mass-Specific BET ^s Surface Area (m ² /g)				
Polystyrene	65	1.05	89.3*	1	0.125, 1	rat	(Brown, Wilson, MacNee, Stone, & Donaldson, 2001)
	202		28.3*	1	0.125, 1		
	535		10.7*	1	0.125, 1		
Titanium Dioxide	20	3.9	50	1.5	0.032, 0.125, 0.5	rat	(Oberdörster et al., 2005)
	250		6.5	0.95	0.125, 0.5, 2		
	20	3.9	50	1.5	0.005, 0.025, 0.1	mouse	(Oberdörster et al., 2005)
	250		6.5	0.95	0.025, 0.1, 0.4		
	300	3.9	6	0.85	0.275, 1.375	rat	(Warheit, Webb, Sayes, Colvin, & Reed, 2006)
	20	3.9	50	1.5	0.125	rat	(Dick, Brown, Donaldson, & Stone, 2003)
	25		50	1.2	1, 6	rat	(Hohr et al., 2002)
Hydrophobic (methylation)	25		50	1.2	1, 6		
	180		6.5	0.85	1, 6		
Carbonaceous materials							
Printex 90	14	2	272	0.79	0.184	rat	(Lu et al., 2009)
				0.79	0.125	rat	(Dick et al.,

				0.79	0.005, 0.02, 0.05	mouse	2003) Stoeger 2006 (T. Stoeger et al., 2006)
5 other types of carbonaceous materials ^{%%}	9, 11, 12, 25, 51	2	800, 441, 268, 108, 43	0.42, 0.62, 0.93, 1.1, 1.4	0.005, 0.02, 0.05	mouse	(T. Stoeger et al., 2006)
Transition metal oxides							
Co ₃ O ₄ -nano	20	---	37	---	0.125	rat	(Dick et al., 2003)
Ni-nano	20	---	36	---	0.125		
ZnO-nano	60	5.6	12.1	1.5	0.25, 1.25	rat	(Sayes, Reed, & Warheit, 2007)
ZnO-fine	--%	5.6	9.6	---	0.25, 1.25		
Silica							
Nanoquartz ^{§§}	12, 50	2.65	91, 31	2.1, 1.4	0.275, 1.375	rat	(Warheit et al., 2007)

568 [§] Surface area characterized by gas adsorption according to the method described by Brunauer, Emmet
569 and Teller (Brunauer et al., 1938)

570 ^{§§} α -crystalline silica (SiO₂); was synthesized hydrothermally in NaOH and not mined and milled as most
571 commercially available quartz types (e.g. Min-U-Sil)

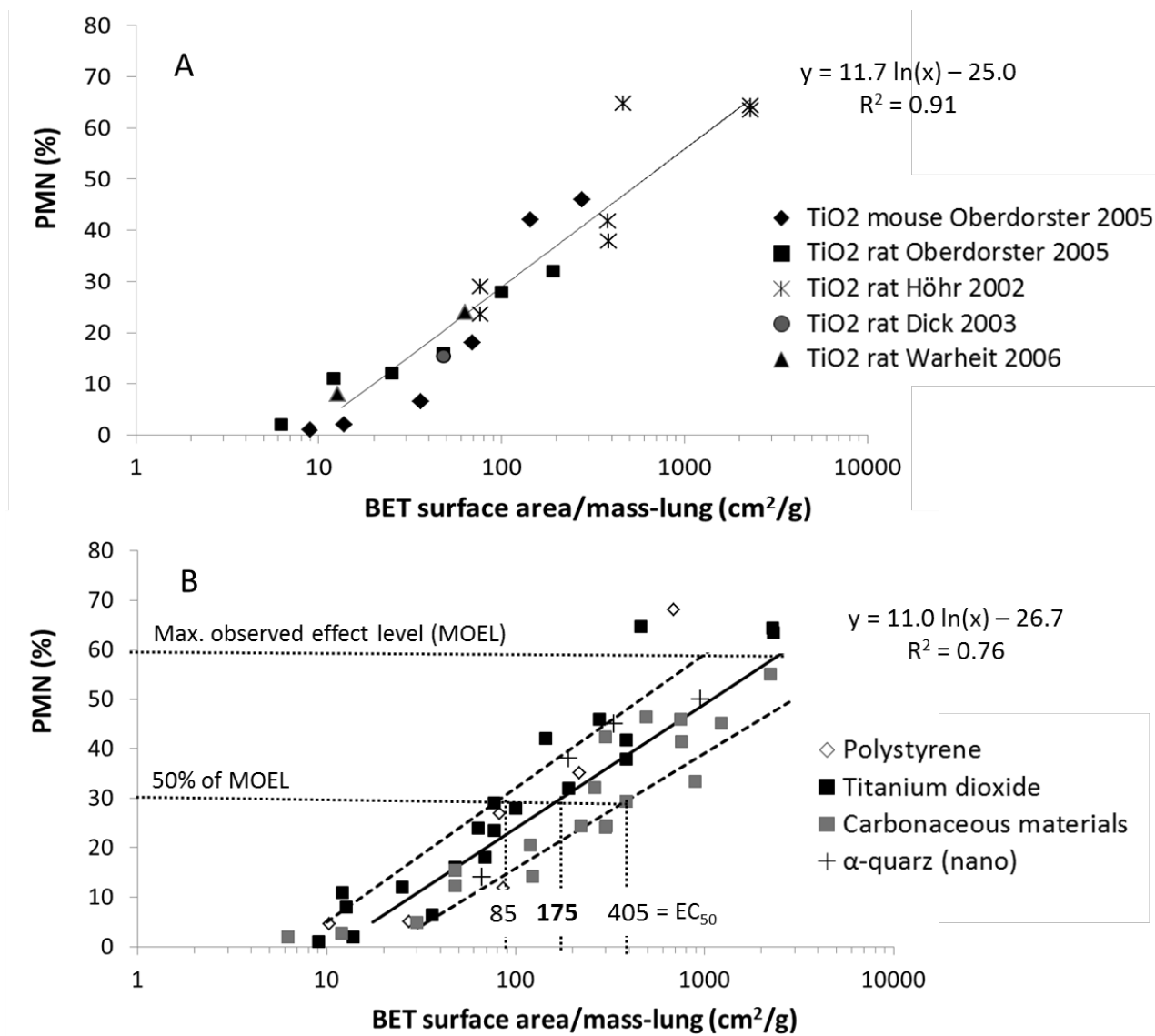
572 [%] diameter of ca. 1000 nm according to manufacturer's information; however, since the accuracy is
573 uncertain, it was not included in analysis of dose metrics relying on primary particle diameter for
574 calculation of number, joint length, geometric surface area

575 ^{%%} In addition to Printex90 (carbon black), spark-discharge generated elemental carbon as well as four
576 other types of combustion-derived soot types were investigated, namely PrintexG (carbon black), Diesel
577 exhaust particles, gas flame soot with low and high organic carbon content.

578 [§] The BET surface area was calculated from the geometric diameter

579

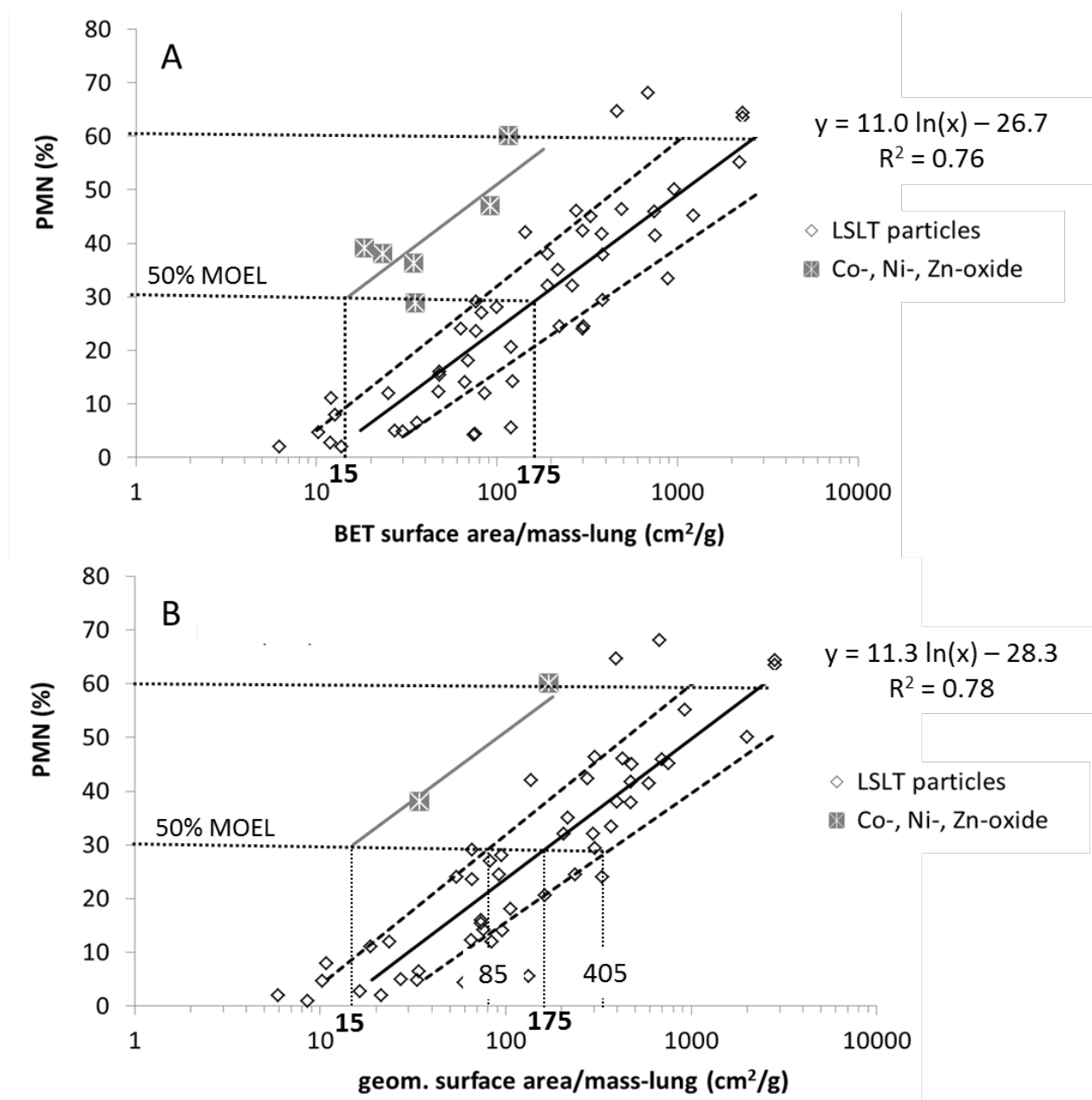
580



581

582 **Fig. 1.** Dependence of acute lung inflammation on BET surface area dose for various types of
 583 nanoparticles (NPs). Lung inflammation is expressed in terms of the number of inflammatory cells
 584 (PMNs, normalized to total number of cells) recovered from the lung 16-24h after intratracheal
 585 instillation of NPs into the lung. **A)** Allometric scaling of mouse and rat data provides consistent results
 586 unifying five different TiO₂ data sets ($R^2 = 0.91$). Inter-species and inter-laboratory differences in the
 587 dose-response curves are reasonably small as indicated by the tight clustering of all data about the fit
 588 line. **B)** Four different types of low-solubility, low-toxicity (LSLT) materials show relatively tight clustering
 589 of the dose-response curves (dashed lines indicate the $\pm 1\sigma$ levels of (solid) best fit line). In spite of
 590 significant differences in primary particle diameter and mass-specific BET surface area (see Table 1)
 591 there is good correlation between inflammation and logarithmic BET surface area dose ($R^2 = 0.76$). The
 592 EC_{50} dose (dose inducing 50% of the maximum observed effect level (MOEL); here: 30% PMN) is
 593 $175 \text{ cm}^2/\text{g-lung}$ (geometric mean; 85 and $405 \text{ cm}^2/\text{g-lung}$ corresponds to $\pm 1\sigma$ dose levels).

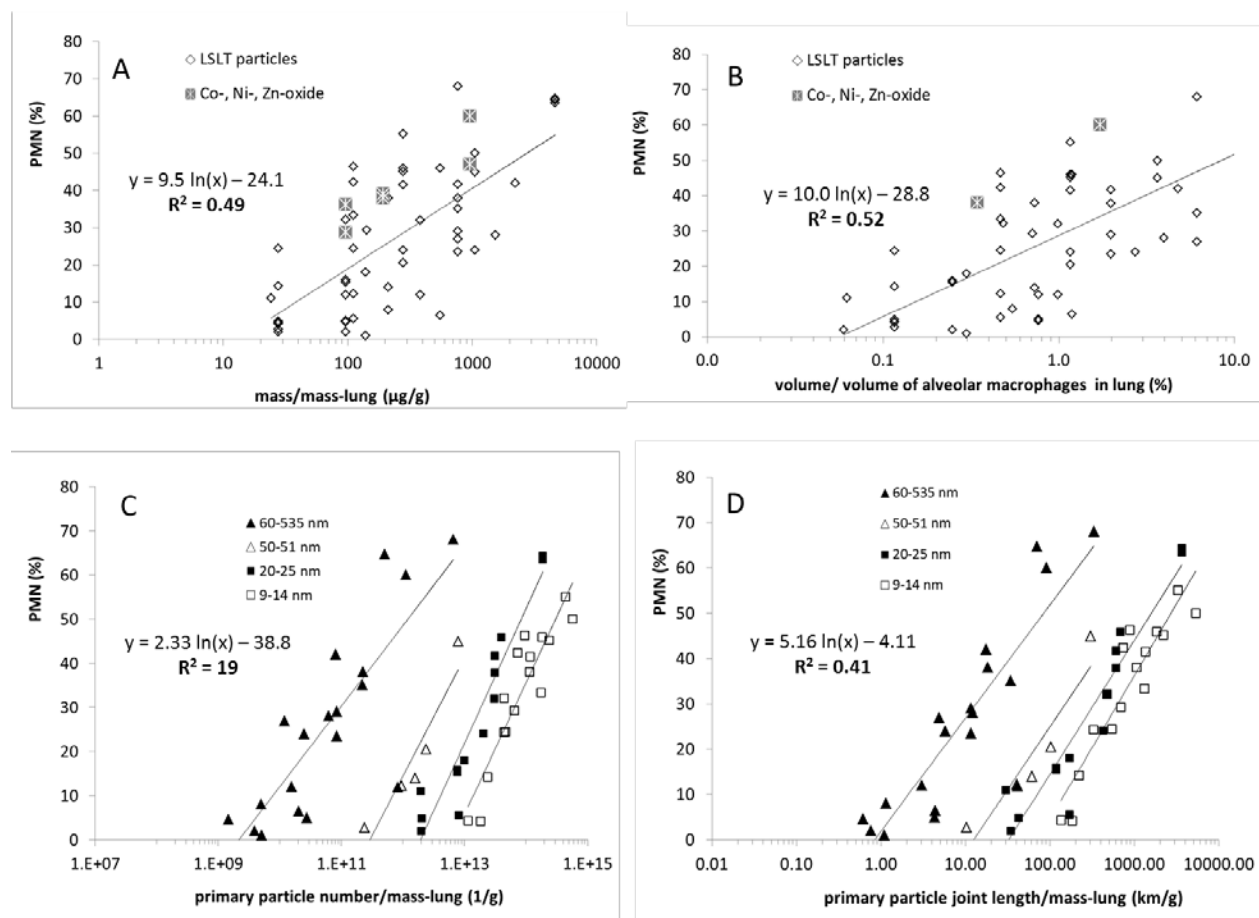
594



595

596 **Fig. 2.** Comparison of acute lung inflammation induced by low-solubility, low-toxicity (LSLT, see Figure
 597 1B) and transition metal oxide NPs (here cobalt, nickel and zinc) with BET or geometric surface area as
 598 dose metric. For both BET surface area **(A)** and geometric surface area **(B)** as the dose metric, transition
 599 metal oxides show a 12-fold elevated toxicity compared to the LSLT particles as evidenced by
 600 corresponding EC_{50} values of 175 cm²/g-lung (with 85 and 405 cm²/g-lung as $\pm 1\sigma$ limits) and 15 cm²/g-
 601 lung, respectively.

602



603

604 **Fig. 3.** Acute lung inflammation data from Figure 2 presented in terms of four different dose metrics. **A)**
 605 **and B)** Mass and volume (normalized to macrophage volume) show a moderately good correlation with
 606 inflammation ($R^2 = 0.49$ and $R^2 = 0.52$, respectively), but – in contrast to surface area – there is no clear
 607 distinction between the toxicity of LSLT and transition metal oxide NPs possible. **C) and D)** For number
 608 and joint length of the primary particles as the dose metric, the correlation with inflammation reduces
 609 to $R^2 = 0.19$ and 0.41 , respectively, (only LSLT data are considered). Moreover, the data suggest an
 610 enhanced toxicity of larger particles (size-stratification indicated by solid lines), which is a metric-related
 611 bias due to the increase in surface area per particle for larger particles.

612